Vol 18 No 11, November 2009
1674-1056/2009/18(11)/4815-08

Chinese Physics B

© 2009 Chin. Phys. Soc.
and IOP Publishing Ltd

Jet-like structures in photoelectron angular distributions*

Wang Yi(王 懿)[a)b)], Zhang Jing-Tao(张敬涛)[a)†],
Ren Xiang-He(任向河)[a)], and Xu Zhi-Zhan(徐至展)[a)]

[a)] *State Key Laboratory of High-field Laser Physics, Shanghai Institute of Optics and Fine Mechanics, Chinese Academy of Sciences, Shanghai* 201800, *China*

[b)] *Graduate School of Chinese Academy of Sciences, Beijing* 100049, *China*

(Received 19 November 2008; revised manuscript received 20 May 2009)

The photoelectron angular distributions (PADs) of hydrogen atoms in an intense laser field of linear polarization are studied using the S-matrix theory in the length gauge. The PADs show main lobes along the laser polarization and jet-like structures sticking from the waist of main lobes. Our previous prediction, based on a nonperturbative scattering theory of photoionization developed by Guo *et al*, showing that the number of jets on one side of PADs may increase by one, three, or other odd numbers and may decrease by one when one more photon is absorbed, is confirmed by this treatment. Within the strong-field approximation, good agreement is obtained between these two quite different treatments. We further study the influence of the Coulomb attraction to PADs, by taking a Coulomb–Volkov state as the continuum state of photoelectrons. We find that under the influence of the Coulomb attraction, the PADs change greatly but the predicted phenomena still appear. This study verifies that the jet-like structures have no relation with the angular momentum of photoelectrons.

Keywords: multiphoton ionization, photoelectron angular distributions, S-matrix theory, Coulomb–Volkov state

PACC: 3280K, 3280F, 3280P

1. Introduction

The study of photoelectron angular distributions (PADs) of above-threshold ionization (ATI) is an attractive area of research, both experimentally and theoretically.[1−3] Experimentally, the PADs of ATI are a direct measure of the physical processes involved in strong-field ionization. The PADs also permit the derivation of other significant data, such as the partial and the total rates. Detailed theoretical studies on PADs are important in understanding the relevant physical processes. Comparisons between theoretical results and experimental measurements offer stringent tests of various extant strong-field-ionization models.

In 1998, Nandor *et al* [4] and Schyja *et al* [5] observed a jet-like structure sticking out from the main lobes in the PADs of low-energy ATI peaks. Here, the main lobes in PADs are the formations of photoelectrons emitted in and around the direction of laser polarization, and the jets are the formations of photoelectrons emitted from the waist between two main lobes. It was found that in a set of ATI peaks when the absorbed-photon number increases by one, the number of jets also increases by one. (Throughout this paper the number of jets denotes that on one side of PADs.) Since in traditional perturbation theory, one photon absorption will alter the electron angular momentum state, it is likely to attribute the number of jets in PADs to the quantum number of the electron angular momentum state. However, the nonperturbative scattering theory for photoionization derived by Guo, Åberg and Crasemann (GAC)[6] revealed that the jet-like structures in PADs have no relation with the angular momentum of photoelectrons.[7] The GAC theory used a generalized phased Bessel (GPB) function to describe the photonic transition amplitude, and found that the jet-like structures are just caused by the extrema of the GPB function.

The GAC theory has had a notable success in explaining strong-field phenomena, such as the angular distribution splitting observed by Bucksbaum *et al*,[8,9] the disappearance of main lobes observed by Richle *et al*,[10,11] and the variation of PADs with laser intensity and frequency.[12] The advantage of us-

*Project supported by the Rising Star Programme of Shanghai, the National Natural Science Foundation of China (Grant No 10774153) and the National Key Basic Research Program of China (Grant No 2006CD806000).

†Corresponding author. E-mail: jtzhang@siom.ac.cn

ing GAC theory to interpret PADs lies in its simplicity and ability to reproduce the PAD patterns observed in experiments. In GAC theory, the PADs are described by a single special function, not a superposition of a set of special functions. This theory shows: (i) the PADs are uniquely determined by the GPB function, (ii) the jets feature the maxima of the GPB function and the number of jets follows a number rule derived by the theory, and (iii) all PADs in different laser frequencies, laser intensities, and atomic binding energies are related by a scaling law.[13] The strong-laser-field phenomena in the nonrelativistic regime were attributed to three basic dimensionless parameters: atomic binding number, ponderomotive number, and absorbed-photon number. With these parameters a scaling law for PADs was established, which still holds in the few-cycle regime.[14,15]

Recently, Bai *et al* [12] extended our previous study to photoionization of hydrogen atoms in an intense laser field and found that the number of jets on one side of PADs may increase by one, three, or other odd numbers after one-more-photon absorption. By varying the laser frequency, the number of jets may decrease by one when one more photon is absorbed.[16] Since the PADs have been detected with high resolutions at present, a frequently asked question is why the predicted phenomena were not observed experimentally. Meanwhile, since there are many strong-field theories of photoionization, should the predicted phenomena be found in other treatments? If the predicted phenomena were confirmed by other strong-field theories, it still provides a strong support to the statement.

In a recent paper,[17] based on the S-matrix theory in the length gauge, we studied theoretically the photoionization process of hydrogen atoms in intense laser fields. In order to take the Coulomb attraction of the parent core into account, we treated the electronic continuum state as the Coulomb–Volkov (CV) state introduced in Ref.[18], instead of the Volkov state used in the GAC theory, and the PADs in various laser fields were obtained. The PADs show the main lobes and the jet-like structures with their number varying with the laser intensity and the kinetic energy of photoelectrons.

Based on our previous studies, in this paper we perform detailed studies on the PADs of hydrogen atoms in an intense laser field of linear polarization and compare the PADs obtained in these two different treatments. For comparison, we first obtain the PADs within the strong-field approximation (SFA) where the Coulomb attraction for the photoelectrons is neglected completely and the electronic continuum state is treated as the Volkov state which describes the motion of a free electron in a laser plane-wave, then compare them with that obtained by GAC theory. A good agreement is shown and detailed differences are also found. The physical reason for these phenomena is also presented. Next we study the PADs when the Coulomb attraction is taken into account by treating the electronic continuum state as the CV state. We will show that the predicted phenomena, for example in the PADs of a set of ATI peaks, where the number of jets may increase by one, three or other odd numbers or may decrease by one when one more photon is absorbed, are also recovered. This study suggests that the jet-like structures have no relation with the angular momentum of photoelectrons and provides a strong support to the predicted phenomena and the GAC theory itself.

2. PADs within the strong-field approximation

The vector potential $\boldsymbol{A}(t)$ of a linearly polarized laser field is written as $\boldsymbol{A}(t) = A_0\hat{\epsilon}\cos(\omega t)$, where $\hat{\epsilon}$ is a unit vector denoting the laser polarization. Using the standard S-matrix theory and treating the electronic continuum state as the Volkov state, we formulate the differential ionization rate after l-photon absorption as[17]

$$\frac{\mathrm{d}W_l}{\mathrm{d}\Omega_\mathrm{p}} = \frac{4\pi A_0^2 p_l}{a_0\omega^2}\left|\int_{-\pi}^{\pi}\mathrm{d}\alpha\cos(\alpha)f_l(\alpha)S(\boldsymbol{p}_l,\sin\alpha)\right|^2, \tag{1}$$

where $\mathrm{d}\Omega_\mathrm{p} = \sin\theta_\mathrm{p}\mathrm{d}\theta_\mathrm{p}\mathrm{d}\phi_\mathrm{p}$ is the differential solid angle of photoelectrons, and θ_p and ϕ_p are the scattering angle and the azimuthal angle in momentum space, respectively; a_0 is the Bohr radius, and the function $f_l(\alpha)$ is given by

$$f_l(\alpha) = \exp(\mathrm{i}\,l\alpha - \mathrm{i}\,Z_l\cos\alpha - \mathrm{i}\,\eta\sin(2\alpha)), \tag{2}$$

where

$$Z_l = \frac{eA_0\hat{\epsilon}\cdot\boldsymbol{p}_l}{m_\mathrm{e}\omega},\quad \eta = \frac{e^2A_0^2}{8m_\mathrm{e}\omega}. \tag{3}$$

For hydrogen atoms in the ground state $|100\rangle$, the function $S(\boldsymbol{p}_l,\sin\alpha)$ for the Volkov states reads[19]

$$S(\boldsymbol{p}_l,\sin\alpha) = \frac{-\mathrm{i}(2a_0)^{7/2}(\boldsymbol{p}_l + eA_0\sin(\alpha)\hat{\epsilon})\cdot\hat{\epsilon}}{\pi[1+a_0^2(\boldsymbol{p}_l+eA_0\sin(\alpha)\hat{\epsilon})^2]^3}, \tag{4}$$

where $\boldsymbol{p}_l$ is the momentum of photoelectrons that satisfies

$$\frac{\boldsymbol{p}_l^2}{2m_\mathrm{e}} = (l - u_\mathrm{p})\omega - I_\mathrm{p}, \tag{5}$$

in which $u_\mathrm{p}\omega$ is the ponderomotive energy and I_p is the ionization potential of the target atoms.

The PADs are calculated according to Eq.(1) by setting $\theta_\mathrm{p} = \pi/2$ and varying ϕ_p from 0 to 2π. Generally, the calculated PADs show main lobes along the laser polarization and jet-like structures sticking out from the waist of the main lobes. The main lobes may split and disappear, and the jets may be greater than the main lobes.

For convenience of comparison, in Fig.1 we depict the PADs calculated according to the ionization-rate formula in Eq.(1). The linearly polarized driving laser is chosen the same as that used in Fig.1 of Ref.[16], say for laser intensity 1.5×10^{13} W/cm^2 and wavelength 700 nm. The calculated PADs show the main lobes and the jet-like structures, and the numbers of jets for this set of ATI peaks are, respectively, 5, 6 and 7, which is the same as that shown in Fig.1 of Ref.[16]. Generally, the calculated PADs agree well with those calculated according to the GAC theory. All the PADs in both treatments show main lobes and jet-like structures, and the numbers of jets are the same. Detailed differences also appear. For example, the jets in the present treatments are generally smaller than those shown in Ref.[16]. Another difference lies in the PAD of the fourth ATI peak, in which the main lobes split badly in the present treatment. However, the overall agreement of PADs is good.

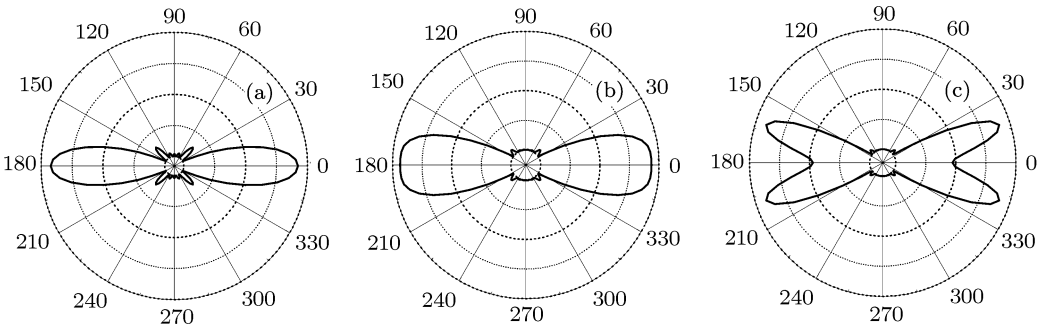


Fig.1. Polar plots of the calculated PADs using the Volkov state. Panels (a), (b) and (c) are for the second, the third and the fourth ATI peaks, respectively. The laser field is of intensity 1.5×10^{13} W/cm^2 and wavelength 700 nm.

As an important result, Ref.[16] predicted that the number of jets may increase by three when one more photon is absorbed. To confirm this prediction, we calculate the PADs under the same conditions as used in Fig.2 of Ref.[16] and the comparison is shown in Fig.2. Like that obtained by the GAC theory, no jet appears in the calculated PAD of the first ATI peak, and three and six jets in the PADs of the second and the third ATI peaks, respectively. For the PAD of the fourth ATI peak, only four jets are visible, and the remaining three jets are too small to be clearly seen. Although there still exist many detailed differences, for example, the main lobes shown in Fig.2(c) are much higher than those in Ref.[16] and the jets are generally smaller than those in Ref.[16], the present calculations show good qualitative agreement with our previous results. We also calculate the PADs under the same conditions as those used in Fig.3 of Ref.[16] and confirm the previous results.

The predicted phenomena were confirmed by a quite different treatment, since the GAC theory differs largely from the present S-matrix treatment in many aspects. The GAC theory is a nonperturbative scattering theory based on the exact solution of laser–electron interaction in the velocity gauge, which has been derived in the frame of the formal scattering theory and obtains an analytical formula of the ionization rate for atoms in intense laser fields. In the ionization-rate formula, the initial wavefunction is separated from the dynamic part of the electronic transition. The S-matrix theory used in the present paper is in the length gauge in which the interaction

depends on the position vector of the electrons. The initial wavefunction incorporates the dynamic part of the electronic transition. Although there are other important differences, they are not related to the present study and not mentioned here. In addition to these differences, we should mention that they are all of the nonperturbative theory of photoionization. Then, what does the similarity of the PADs obtained by these two different treatments imply? Where do the differences in the PADs come from?

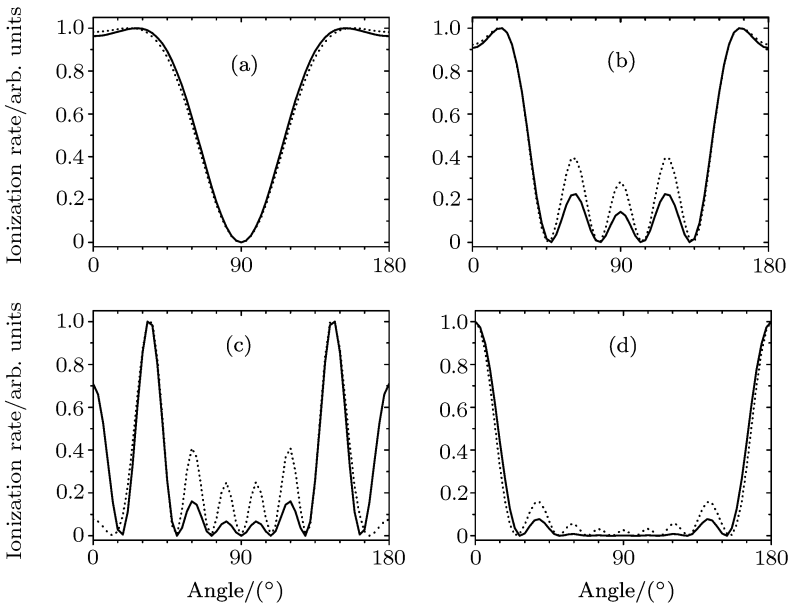


Fig.2. The calculated PADs using the Volkov states. Figures (a), (b), (c) and (d) are for the first, the second, the third, and the fourth ATI peaks. The laser field is of intensity 10^{13} W/cm^2 and wavelength 780 nm.[20] For convenience of comparison, each PAD is normalized by its maximum. The solid lines are for the present calculation, and the dotted lines are for the GAC results.

The GAC theory interprets PADs in terms of the GPB function defined as follows:

$$\mathcal{X}_{-l}(Z_l,\eta) \equiv \sum_{m=-\infty}^{\infty} \mathrm{X}_{-l-2m}(Z_l)\mathrm{X}_m(\eta), \qquad (6)$$

where the phased Bessel functions $\mathrm{X}_n(z)$ of a complex variable z are related to the ordinary Bessel functions $\mathrm{J}_n(r)$ by

$$\mathrm{X}_n(z) = \mathrm{J}_n(r)\mathrm{e}^{\mathrm{i}\,n\varphi}, \quad (z = r\mathrm{e}^{\mathrm{i}\,\varphi}). \qquad (7)$$

For a linearly polarized laser field, both Z_l and η are real, then the GPB function reduces to

$$\mathcal{X}_{-l}(Z_l,\eta) \equiv \sum_{m=-\infty}^{\infty} \mathrm{J}_{-l-2m}(Z_l)\,\mathrm{J}_m(\eta), \qquad (8)$$

where the two variables are given in Eq.(3). The value of the GPB function increases oscillatorily as Z_l increases, and the oscillation pattern depends on the value of η. The oscillation of the GPB function forms the jet-like structures in PADs, and the number of jets is twice the extrema of the GPB function in the domain of $Z_{l\,\max}$.[7] The ionization-rate formula in Eq.(1) can be rewritten as

$$\frac{\mathrm{d}W_l}{\mathrm{d}\Omega_\mathrm{p}} = \frac{4\pi A_0^2 p_l}{a_0\omega^2}\left|\sum_{n,m}(\mathrm{i})^n \mathrm{J}_n(-Z_l)\mathrm{J}_m(\eta)\int_{-\pi}^{\pi}\mathrm{d}\alpha\cos(\alpha)\exp\left[\mathrm{i}(l+n-2m)\alpha\right]S(\boldsymbol{p}_l,\alpha)\right|^2$$
$$= \frac{4\pi A_0^2 p_l}{a_0\omega^2}\left|\sum_{j,m}(\mathrm{i})^j(-1)^j \mathrm{J}_{j+2m}(Z_l)\mathrm{J}_m(-\eta)\int_{-\pi}^{\pi}\mathrm{d}\alpha\cos(\alpha)\exp[\mathrm{i}(l+j)\alpha]S(\boldsymbol{p}_l,\alpha)\right|^2$$
$$= \frac{4\pi A_0^2 p_l}{a_0\omega^2}\left|\sum_{j}(\mathrm{i})^j(-1)^j \mathcal{X}_j(Z_l,\eta)\int_{-\pi}^{\pi}\mathrm{d}\alpha\cos(\alpha)\exp[\mathrm{i}(l+j)\alpha]S(\boldsymbol{p}_l,\alpha)\right|^2. \quad (9)$$

Clearly, the GPB function also appears in the ionization-rate formula. The subscript j denotes a possible transition channel, thus summing over j means that many transition channels can contribute to the same ATI peak. Numerical calculations show that the integration over α becomes notable when $l+j$ is an odd number. Since $\exp[\mathrm{i}(l+j)\alpha]$ oscillates quickly for large values of $j+l$, only several channels may contribute dominantly to the overall ionization rate, implying that only several GPB functions are involved in forming an ATI peak. This is the reason why good agreement is obtained between the PADs calculated by the GAC theory and those by the present treatment, and the interference between multiple ionization channels in the present treatment causes the differences in the calculated PADs.

3. PADs with the Coulomb potential included

Since the Volkov state describes a free electron interacting with a laser plane wave, the use of the Volkov state means that the Coulomb attraction of the parent core to the photoelectrons is completely neglected. In reality, however, due to the long-range nature of the Coulomb attraction, an electron will interact with a laser field under the influence of the Coulomb attraction. It has been shown that the Coulomb potential affects the broadness of the main lobes and the number of jets.[17] Then, a question arises: What will the PADs become when the influence of the Coulomb potential is taken into account?

In order to look for an answer, we treat the state of photoelectron as the CV state introduced by Jain and Tzoar[18] and perform the Coulomb-corrected S-matrix treatment to obtain the ionization-rate formula.[20] (For details see also Ref.[17].) In the CV state, the laser field and the Coulomb field are treated on an equal footing and the influence of the Coulomb potential is determined by the momentum of photoelectrons in such a manner that the low-energy electrons are influenced strongly while the high-energy electrons are weakly affected. Following the standard S-matrix treatment, and treating the electronic continuum state as the CV state, the differential ionization rate after l-photon absorption is worked out to be

$$\frac{\mathrm{d}W_l}{\mathrm{d}\Omega_\mathrm{p}} = \frac{2^8 a_0^3 A_0^2}{\omega^2\left[1-\exp(-2\pi v)\right]}\left|\int_{-\pi}^{\pi}\mathrm{d}\alpha\cos(\alpha)f_l(\alpha)S'(\boldsymbol{p}_l,\sin\alpha)\right|^2, \quad (10)$$

where

$$S'(\boldsymbol{p}_l,\sin\alpha) = \frac{(1-\mathrm{i}\,v)M^{\mathrm{i}\,v}\hat{\epsilon}\cdot[eA_0\sin(\alpha)\hat{\epsilon}A+\boldsymbol{p}_l B]}{\{1+a_0^2[eA_0\sin(\alpha)\hat{\epsilon}+\boldsymbol{p}_l]^2\}^3}, \quad (11)$$

in which the coefficients are given by

$$A = [-(2\,\mathrm{i}+v)+(2v-\mathrm{i})M+\frac{(v-\mathrm{i})}{1-\mathrm{i}\,v}(1+\mathrm{i}\,v)M^2], \quad (12)$$

$$B = [2\,\mathrm{i}+v-(v-\mathrm{i})M], \quad (13)$$

$$M = \frac{\{1+[eA_0\sin(\alpha)\hat{\epsilon}+\boldsymbol{p}_l]^2 a_0^2\}}{[(eA_0\sin(\alpha))^2 a_0^2-(p_l a_0+\mathrm{i})^2]}, \quad (14)$$

with v being calculated as $v = 1/(a_0 p_l)$. Other quantities are the same as those for the Volkov state. According to this formula, we calculate the PADs under the influence of Coulomb attraction. The calculated PADs clearly show main lobes and jet-like structures.

In order to show the influence of the Coulomb potential, in Fig.3 we depict several PADs using the CV state, under the same conditions as for the Volkov state shown in Fig.2. Distinctive differences appear between the PAD using the Volkov state and that using the CV state. For example, for the first ATI peak, the main lobes of the PAD using the Volkov state are broad and split slightly and no jet appears, while the main lobes do not show any split and two jets appear on each side of the PAD for the CV state. The number of jets in the PAD using the CV state also differs from that using the Volkov states. In addition to these discrepancies, we note that five jets appear on one side of the PAD for the second ATI peak, which implies that the number of jets increases by three when one more photon is absorbed. This feature agrees well with our previous prediction. For other higher order ATI peaks, one more jet appears when one more photon is absorbed. We should mention that, in the present treatment, the calculated PADs for even-photon processes always have a central jet, while those for odd-photon processes do not show any central jet. Meanwhile, the number of jets does not increase by two or other even numbers when one more photon is absorbed. These features also agree with our previous results based on the GAC theory.[7]

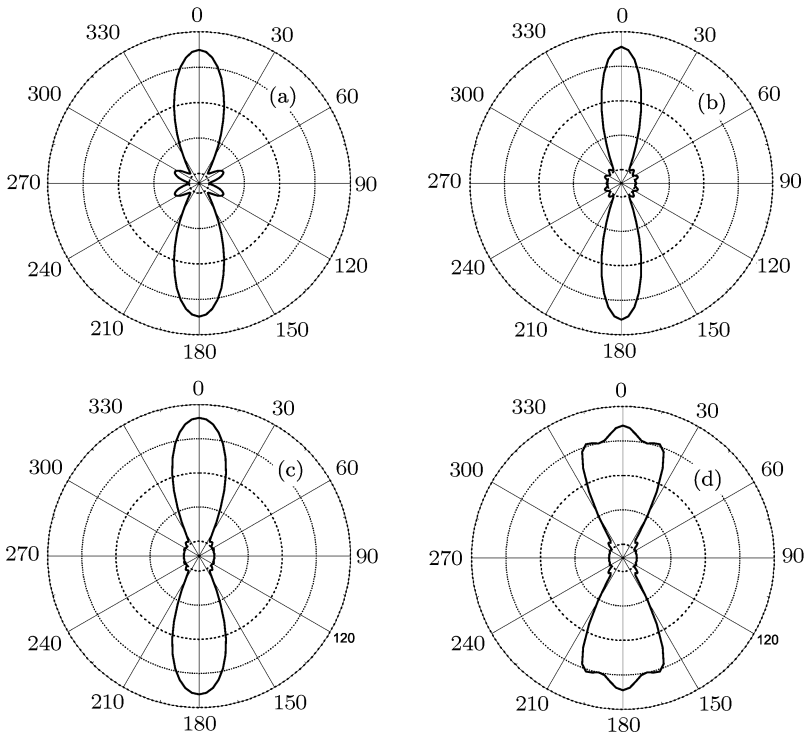


Fig.3. Polar plots of the calculated PADs using the Coulomb–Volkov state. Other conditions are the same as those in Fig.2.

Our calculations also show that the number of jets may decrease by one when one more photon is absorbed. Figure 4 depicts the PADs for the first six ATI peaks at laser intensity 5×10^{13} W/cm^2. Four jets, two of which are large while the other two are small but still notable, appear on each side of the PAD for the first ATI peak. Five jets appear on one side of the PAD of the second peak. The PADs for the following three ATI peaks are highly peaked along the polarization vector. Detailed study discloses that there are 8, 9 and 10 jets on each side of the PADs for the 3rd, 4th and 5th ATI peaks, respectively. However, in the PAD of the sixth ATI peak, there are only 9 jets on one side of the PAD, suggesting that the number of jets decreases by one with one-more-photon absorption. The decrease with one-more-photon absorption, as well as the change in the

number of jets in the CV treatment, is caused by the minimum of the space integration ($S(p, \sin(\alpha))$ in Eq.(27) of Ref.[17]) matrix, resulting from the irregularity of the CV states. When a maximum of the GPB function meets a minimum of $S(p, \sin(\alpha))$, a jet disappears.

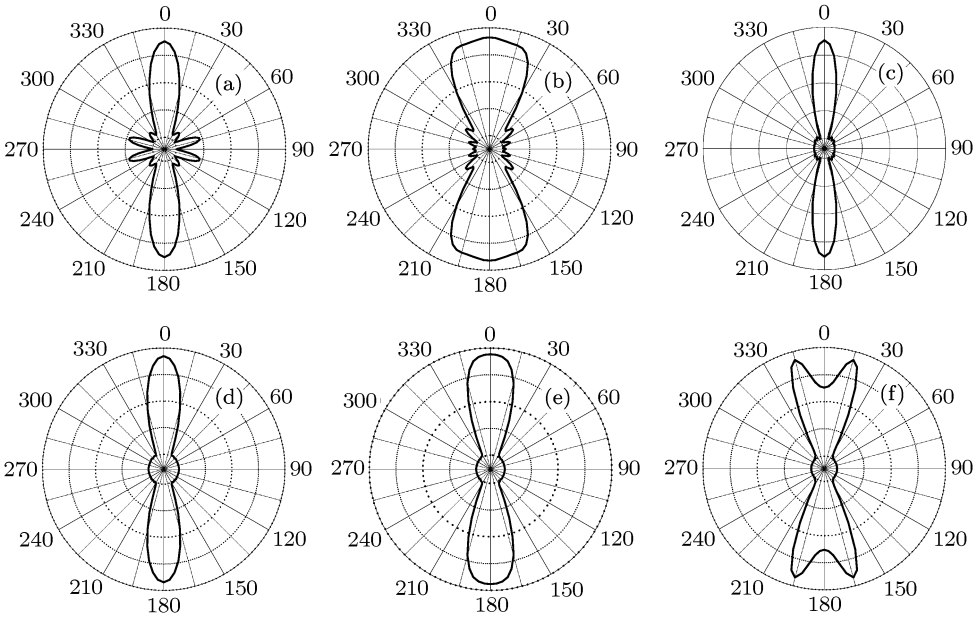


Fig.4. Polar plots of the calculated PADs using the Coulomb–Volkov state. Figures (a)–(f) are for the first six ATI peaks. The laser field is of intensity 5×10^{13} W/cm^2 and wavelength 800 nm.

The phenomenon that the number of jets may increase by one, three or other odd numbers and may decrease by one when one more photon is absorbed occurs over a wide laser intensity range. Our calculations indicate that at higher intensities, the predicted changes in the number of jets are quite general. For example, at laser intensity 3×10^{14} W/cm^2, the number of jets in the PADs of the first six ATI peaks is, respectively, 4, 7, 10, 13, 14, and 15. A five-jet-increase case also appears in our calculations.

For convenience of experimental observation, it will be useful to choose a proper laser intensity to observe the predicted phenomena. On one hand, since the photoelectron rate increases nonlinearly with laser intensity, it is helpful to the experimental observations to take a higher laser intensity. On the other hand, high-intensity PADs have many jets, but only several jets are visible, while others are too small to be seen clearly. More importantly, if the peak intensity of the laser field is too high, ionization will occur over a wide intensity range, and the PADs at different intensities will incorporate into each other which may obstruct their predicted features. Such a case has occurred in the tunneling ionization where the Keldysh parameter $\gamma = \sqrt{I_{\rm p}/2u_p\omega} < 1$ and the peak structure in the photoelectrons' energy spectrum disappears. Thus, increasing the laser intensity is not always advantageous to the experimental observations. Here we suggest that to observe the predicted phenomena, the laser intensity should be lower than 10^{14} W/cm^2 to ensure that the Keldysh parameter $\gamma > 1$ where the photoelectron spectrum shows well-separated peaks.

4. Conclusion

Our previous prediction, based on the nonperturbative scattering theory of photoionization, that the number of jets may increase by one, three, or other odd numbers or may decrease by one when one more photon is absorbed, is confirmed by the S-matrix theory in the length gauge. Good qualitative agreement is obtained by the two kinds of quite different treatments within the SFA. When the Coulomb potential is taken into account, by treating the continuum state of photoelectrons as the CV state, the pattern of PADs changes greatly but the predicted change in the num-

ber of jets still appears. This study verifies that the number of jets has no relation with the angular momentum of photoelectrons. This study also provides strong support to the interpretation of PADs in terms of the GPB function. Actually, the amplitude of a photonic transition expressed by a generalized Bessel function is a common feature for many nonperturbative photoionization theories, such as in the well-known formula given by Reiss.[21] The distinctive differences between PADs with and without the SFA imply that the results based on the SFA become more accurate when Coulomb attraction plays a minor role.

References

[1] Milosevic D B, Paulus G G, Bauer D and Becker W 2006 *J. Phys.* B **39** R203
[2] Li C P and Zhou X X 2007 *Chin. Phys.* **16** 605
[3] Hu X Q, Xu J, Luo G and Ma Y 2007 *Chin. Phys.* **16** 3631
[4] Nandor M J, Walker M A and van Woerkom L D 1998 *J. Phys.* B **31** 4617
[5] Schyja V, Lang T and Helm H 1998 *Phys. Rev.* A **57** 3692
[6] Guo D S, Åberg T and Crasemann B 1989 *Phys. Rev.* A **40** 4997
Gao J, Guo D S and Wu Y S 2000 *Phys. Rev.* A **61** 043406
[7] Zhang J T, Zhang W Q, Xu Z Z, Li X F, Fu P M, Guo D S and Freeman R R 2002 *J. Phys.* B **35** 4809
[8] Bucksbaum P H, Schumacher D W and Bashkansky M 1988 *Phys. Rev. Lett.* **61** 1182
[9] Guo D S and Drake G W F 1992 *Phys. Rev.* A **45** 6622
[10] Reichle R, Helm H and Kiyan I Y 2001 *Phys. Rev. Lett.* **87** 243001
[11] Zhang J T, Van Woerkom L D, Guo D S and Freeman R R 2007 *Phys. Rev.* A **76** 015401
[12] Bai L H, Zhang J T, Zhang X M and Xu Z Z 2006 *Phys. Rev.* A **74** 025402
[13] Guo D S, Zhang J T, Xu Z Z, Li X F, Fu P M and Freeman R R 2003 *Phys. Rev.* A **68** 043404
[14] Zhang J T, Bai L H, Gong S Q, Xu Z Z and Guo D S 2007 *Opt. Express* **15** 7261
[15] Zhang X M, Zhang J T, Bai L H, Gong Q H and Xu Z Z 2005 *Opt. Express* **13** 8708
[16] Bai L H, Zhang J T, Xu Z Z and Guo D S 2006 *Phys. Rev. Lett.* **97** 193002
[17] Zhang J T and Nakajima T 2007 *Phys. Rev.* A **75** 043403
[18] Jain M and Tzoar N 1978 *Phys. Rev.* A **18** 538
[19] Becker A, Plaja L, Moreno P, Nurhuda M and Faisal F H M 2001 *Phys. Rev.* A **64** 023408
[20] Leone C, Bivona S, Burlon R, Morales F and Ferrante G 1989 *Phys. Rev.* A **40** 1828
[21] Reiss H R 1980 *Phys. Rev.* A **22** 1786